Multiscale time integration of dissipative thermodynamics with energy-momentum consistent TFEM

Michael Groß

Chair of Applied Mechanics/Dynamics

Chemnitz University of Technology

September 10, 2012

ECCOMAS 2012

MS626-2: Multiphysics simulation

Multiscale time integration in coupled problems

Felippa & Park [2004], Markovic et al. [2005], Matthies, Niekamp & Steindorf [2006], Kassiotis, Colliat, Ibrahimbegovic & Matthies [2009]

1 Finite difference methods in time (partitioned strategy)

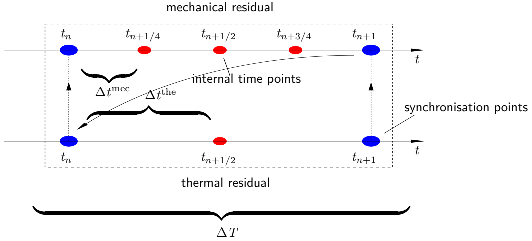

(see Kassiotis, Colliat, Ibrahimbegovic & Matthies [2009])

2 Finite element methods in time (monolithic strategy)

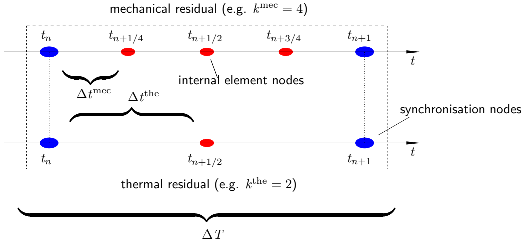

Simulation with different time step sizes

[1] Belytschko & Mullen [1978], Hughes & Liu [1978], Park & Housner [1982], Liu [1983], Smolinski, Belytschko & Neal [1988], Smollinski, Sleith & Belytschko [1996], Smollinski & Wu [1998,2000], Felippa, Park & Farhat [2001], Gravouil & Combescure [2001], Marsden & West [2001], Rugonyi & Bathe [2001], Ibrahimbegovic & Markovic [2003], Ober-Blöbaum & Leyendecker [2011]

[2] Hughes & Hulbert [1988], Masud & Hughes [1997], Bottasso [2002], Larsson, Hansbo & Runesson [2003], Hübner, Walhorn & Dinkler [2004], Michler, Hulshoff, van Brummelen & de Borst [2004], Hansbo, Hermannsson & Svedberg [2004], Tezduyar, Sathe, Schwaab & Conklin [2008]

1. Finite difference methods in time[1]
    - Semi-implicit time integration of non-uniform meshes
        - nodal partitioning
        - element partitioning
    - Mixed time integration (field partitioning) of
        - area and boundary coupled problems
        - problems with inelastic media
        - Multiple timescale problems
2. Finite element methods in time[2]
    - Space-time Galerkin methods
        - solid mechanics
        - fluid flow problems
        - area and boundary coupled field problems
    - Time-discontinuous least squares methods in fluid flow problems
    - Multiple timescale problems

Energy-consistent finite element method in time

French & Schaeffer [1990], Betsch & Steinmann [2000,2001], Larson & Niklasson [2001], Hansbo [2001], Betsch & Steinmann [2002], Cockburn [2003], G. [2004], G., Betsch & Steinmann [2005], Bui [2007], Mohr, Menzel & Steinmann [2008], Bargmann [2008], G. [2009], G. & Betsch [2010,2011]

1. Stability estimate of the relative total energy

$$\frac{\mathrm{d}\mathcal{H}(t)}{\mathrm{d}t} = \int_{\mathscr{B}_0} \frac{\theta_\infty}{\theta_t} D_t^{\mathrm{tot}} \leqslant 0 \qquad \mathcal{H}(t) = \int_{\mathscr{B}_0} \rho_0 \boldsymbol{v}_t \cdot \boldsymbol{v}_t + \psi_t + (\theta_t - \theta_\infty)\,\eta_t$$

2. Energy-consistent finite element method

$$\begin{aligned}\mathcal{H}(T) - \mathcal{H}(t_0) &= \int_{\mathscr{T}}\int_{\mathscr{B}_0} \rho_0 \boldsymbol{v}_t \cdot \frac{\partial \boldsymbol{v}_t}{\partial t} + \int_{\mathscr{T}}\int_{\mathscr{B}_0} \rho_0 \frac{\partial \boldsymbol{v}_t}{\partial t} \cdot \left[\frac{\partial \boldsymbol{\varphi}_t}{\partial t} - \boldsymbol{v}_t\right] \\ &+ \int_{\mathscr{T}}\int_{\mathscr{B}_0} \frac{\partial \psi_t}{\partial \boldsymbol{F}} : \frac{\partial \boldsymbol{F}_t}{\partial t} - \int_{\mathscr{T}}\int_{\mathscr{B}_0} \frac{\partial \boldsymbol{\varphi}_t}{\partial t} \cdot \left[\rho_0 \frac{\partial \boldsymbol{v}_t}{\partial t} - \mathrm{DIV}[\boldsymbol{F}_t \boldsymbol{S}_t]\right] \\ &+ \int_{\mathscr{T}}\int_{\mathscr{B}_0} \frac{\partial \psi_t}{\partial \boldsymbol{C}^{\mathrm{int}}} : \frac{\partial \boldsymbol{C}_t^{\mathrm{int}}}{\partial t} + \int_{\mathscr{T}}\int_{\mathscr{B}_0} \frac{\partial \boldsymbol{C}^{\mathrm{int}}}{\partial t} : \left[\frac{1}{2}[\boldsymbol{C}_t^{\mathrm{int}}]^{-1}\boldsymbol{\Sigma}_t - \boldsymbol{Y}_t\right] \\ &+ \int_{\mathscr{T}}\int_{\mathscr{B}_0} (\theta_t - \theta_\infty) \frac{\partial \eta_t}{\partial t} - \int_{\mathscr{T}}\int_{\mathscr{B}_0} (\theta_t - \theta_\infty)\left[\frac{\partial \eta_t}{\partial t} + \frac{1}{\theta_t}\mathrm{DIV}[\boldsymbol{Q}_t] - \frac{D_t^{\mathrm{int}}}{\theta_t}\right] \\ &\qquad \underbrace{+ \int_{\mathscr{T}}\int_{\mathscr{B}_0} \frac{\partial \theta_t}{\partial t}\left[\frac{\partial \psi_t}{\partial \theta_t} + \eta_t\right] - \int_{\mathscr{T}}\int_{\mathscr{B}_0} \frac{\partial \boldsymbol{F}_t}{\partial t} : \left[\frac{\partial \psi_t}{\partial \boldsymbol{F}_t} - \boldsymbol{F}_t \boldsymbol{S}_t\right]}_{0} \\ &= -\int_{\mathscr{T}}\int_{\mathscr{B}_0} \frac{\theta_\infty}{\theta_t} D_t^{\mathrm{tot}} \leqslant 0\end{aligned}$$

The ehG method

1. Continuous finite elements in space
2. Continuous and discontinuous finite elements in time
   - Continuous for hyperbolic evolution equations
   - Continuous for local evolution equations
   - Discontinuous for parabolic evolution equations
3. Nodal approximations of strain and entropy

$$\boldsymbol{C}_t := \sum_{I=1}^{m_{\text{mec}}} M_I^{\text{mec}}(t)\,\boldsymbol{C}_{t_I} \qquad \eta_t := \sum_{J=1}^{m_{\text{the}}} M_J^{\text{the}}(t)\,\eta_{t_J}$$

4. Enhanced stress and entropy production approximations

$$\boldsymbol{\Sigma}_\alpha^{\text{tot},\flat} := \boldsymbol{\Sigma}_\alpha^{\text{phy},\flat} + \boldsymbol{\Sigma}_\alpha^{\text{alg},\flat} \qquad D_t^{\text{tot}} = D^{\text{phy}} + D_t^{\text{alg}}$$

5. Advantanges
   - Stability as energy-consistent time stepping schemes
   - Higher order accuracy as standard Galerkin methods
6. ...but depends on the considered physical problem

Dynamics of solid inelastic media

Oden [1972], Gurtin [1981], Miehe [1988], Holzapfel [2000], Andrews [2005], Chernyshev [2007], Fernández & Kuttler [2010]

1. Lagrangian local momentum balance

$$\boldsymbol{v}_t := \frac{\partial \boldsymbol{\varphi}_t}{\partial t} \qquad \boxed{\frac{\partial \boldsymbol{v}_t}{\partial t} = \frac{1}{\rho_0}\,\mathrm{DIV}[\boldsymbol{F}_t \boldsymbol{S}_t] + \boldsymbol{b}_t}$$

2. Deformation and strain measures

$$\boldsymbol{F}_t := \mathrm{GRAD}[\boldsymbol{\varphi}_t] \qquad \boldsymbol{C}_t := [\boldsymbol{F}_t^\flat]^T \boldsymbol{F}_t \qquad \boldsymbol{E}_t := \frac{1}{2}\,[\boldsymbol{C}_t - \boldsymbol{I}]$$

3. Piola/Mandel stress tensor

$$\boldsymbol{S}_t := 2\,\frac{\partial \psi_t}{\partial \boldsymbol{C}} \qquad \boldsymbol{\Sigma}_t^\flat := \boldsymbol{C}_t \boldsymbol{S}_t$$

4. Stress power & deformation rate tensor

$$\mathcal{P}_t := \boldsymbol{\Sigma}_t^\flat : \boldsymbol{L}_t^\sharp \qquad \boldsymbol{L}_t^\sharp := \frac{1}{2}\,\boldsymbol{C}_t^{-1} \frac{\partial \boldsymbol{C}}{\partial t}$$

Isotropic finite viscoelasticity

Miehe[1988], Le Tallec et al. [1993], Kaliske [1995], Reese & Govindjee [1998], Reese [2001], Kleuter [2007], Hartmann & Hamkar [2010]

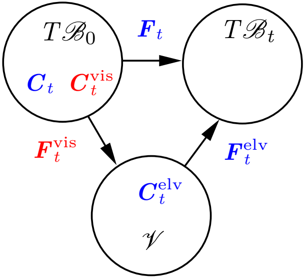

1. Elastic metric tensor

$$\boldsymbol{C}_t^{\text{elv}} := [\boldsymbol{F}_t^{\text{vis}}]^{-T}\,\boldsymbol{C}_t[\boldsymbol{F}_t^{\text{vis}}]^{-1}$$

2. Elastic invariants

$$\mathfrak{I}(\boldsymbol{C}_t^{\text{elv}}) = \mathfrak{I}(\boldsymbol{C}_t\,[\boldsymbol{C}_t^{\text{vis}}]^{-1})$$

3. Viscous internal variable

$$\boldsymbol{C}_t^{\text{vis}} := [\boldsymbol{F}_t^{\text{vis},\flat}]^T\,\boldsymbol{F}_t^{\text{vis}}$$

4. Viscous evolution equation

$$\boxed{\boldsymbol{\Sigma}_t^{\flat} = n_{\text{dim}}\,V_{\text{sph}}\,\textsc{Sph}([\boldsymbol{L}_t^{\text{vis},\sharp}]^T) + 2\,V_{\text{dev}}\,\textsc{Dev}([\boldsymbol{L}_t^{\text{vis},\sharp}]^T)}$$

5. Viscous dissipation/rate tensor

$$D_t^{\text{vis}} := \boldsymbol{\Sigma}_t^{\flat} : \boldsymbol{L}_t^{\text{vis},\sharp} \geqslant 0 \qquad \boldsymbol{L}_t^{\text{vis},\sharp} := \frac{1}{2}\,[\boldsymbol{C}_t^{\text{vis}}]^{-1}\,\frac{\partial \boldsymbol{C}^{\text{vis}}}{\partial t}$$

Thermodynamics of solids

Oden [1972], Miehe [1988], Holzapfel & Simo [1996], Bérardi et al. [1996], Lion [1997], Reese [2000], Boukamel et al. [2001]

1. Lagrangian local entropy balance

$$\eta_t := -\frac{\partial \psi_t}{\partial \theta} \qquad \boxed{\frac{\partial \eta_t}{\partial t} = -\frac{1}{\theta_t}\,\mathrm{DIV}[\boldsymbol{Q}_t] + \frac{D_t^{\mathrm{vis}}}{\theta_t} + \frac{r_t}{\theta_t}}$$

2. Fourierian isotropic heat conduction law

$$\boldsymbol{q}_t := -k_0\,(J_t\,\boldsymbol{F}_t^{\sharp})^{-T}\,\mathrm{GRAD}[\theta_t] \qquad \boldsymbol{Q}_t := J_t\,\boldsymbol{F}_t^{-1}\,\boldsymbol{q}_t$$

3. Specific heat capacity & thermal expansion

$$\theta_t\,\frac{\partial \eta_t}{\partial \theta} =: c \geq 0 \qquad \frac{1}{n_{\mathrm{dim}}}\,\frac{\partial \mathrm{DET}[\boldsymbol{F}_t]}{\partial \theta} =: \beta \geq 0$$

4. Thermal dissipation

$$D_t^{\mathrm{cdu}} := -\mathrm{GRAD}[\ln \theta_t]\cdot \boldsymbol{Q}_t \geq 0$$

Entropy at the thermal time nodes

1. Method 1: L_2-projection of the right Cauchy-Green tensor
   - Entropy approximation at the thermal nodes
   $$\eta_{t_J} := -\frac{\partial\psi(\theta_{t_J}, \boldsymbol{C}_{t_J})}{\partial\theta}$$
   - Right Cauchy-Green tensor at the thermal nodes
   $$\boldsymbol{C}_{\bar{t}_K} \equiv \sum_{I=1}^{m_{\text{mec}}} M_I^{\text{mec}}(\bar{t}_K)\boldsymbol{C}_{t_I} \doteq \sum_{J=1}^{m_{\text{the}}} M_J^{\text{the}}(\bar{t}_K)\boldsymbol{C}_{t_J}$$
   where $\bar{t}_K$, $K = 1, \ldots, M_{\text{the}}$ (thermal quadrature points)
2. Method 2: L_2-projection of the entropy density
$$\sum_{K=1}^{m_{\text{the}}} \frac{\partial\theta_{\bar{t}_K}}{\partial t}\left[\frac{\partial\psi(\theta_{\bar{t}_K}, \boldsymbol{C}_{\bar{t}_K})}{\partial\theta} + \eta_{\bar{t}_K}\right] w_K \doteq 0$$
3. Discrete L_2-projection in time
$$\begin{bmatrix}\boldsymbol{C}_{t_1}\\ \vdots \\ \boldsymbol{C}_{t_{M_{\text{the}}}}\end{bmatrix} := \boldsymbol{W}\otimes\boldsymbol{I}\begin{bmatrix}\boldsymbol{C}_{\bar{t}_1}\\ \vdots \\ \boldsymbol{C}_{\bar{t}_{M_{\text{the}}}}\end{bmatrix} \qquad \begin{bmatrix}\eta_{t_1}\\ \vdots \\ \eta_{t_{M_{\text{the}}}}\end{bmatrix} := -\boldsymbol{W}\begin{bmatrix}\partial_\theta\psi_{\bar{t}_1}\\ \vdots \\ \partial_\theta\psi_{\bar{t}_{M_{\text{the}}}}\end{bmatrix}$$

Current configurations of the flying square

($k^{\text{mec}} = 4, k^{\text{the}} = 4, k^{\text{vis}} = 4$, method 2)

Height	h	$1\,\text{cm}$
Width	b	$1\,\text{cm}$
Thermoviscoelastic Simo-Taylor material		
Mass density	ρ_0	$8.93\,\text{kg/cm}^2$
First Lamé constant	μ	$7.5\,\text{J/cm}^2$
Second Lamé constant	λ	$30\,\text{J/cm}^2$
Deviatoric viscosity	V_{dev}	$10\,\text{kJs/cm}^2$
Spherical viscosity	V_{sph}	$50\,\text{kJs/cm}^2$
Specific heat capacity	c	$0.1\,\text{kJ/cm}^2\text{K}$
Heat expansion coefficient	β	$10^{-4}\,\text{K}^{-1}$
Heat conduction coefficient	k_0	$0.01\,\text{kW/K}$
Ambient temperature	Θ_∞	$298.15\,\text{K}$
Global iteration tolerance	tol	$10^{-6}\,\text{J}$
Local iteration tolerance	tolevo	$10^{-10}\,\text{J/cm}^2$
Maximum number of iterations	maxit	10
Number of spatial elements	n_{el}	4
Number of spatial nodes	n_{no}	9

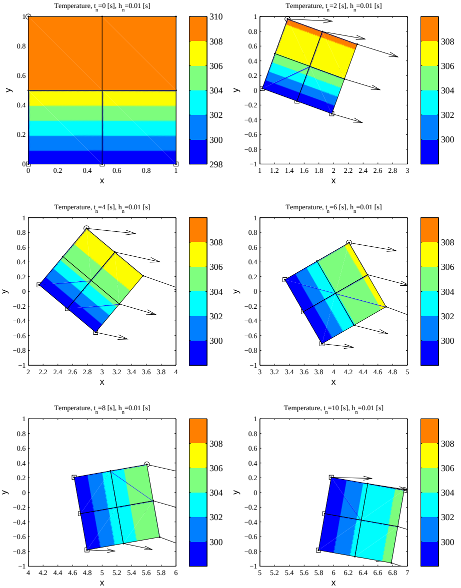

Relative L_2-error of the flying square

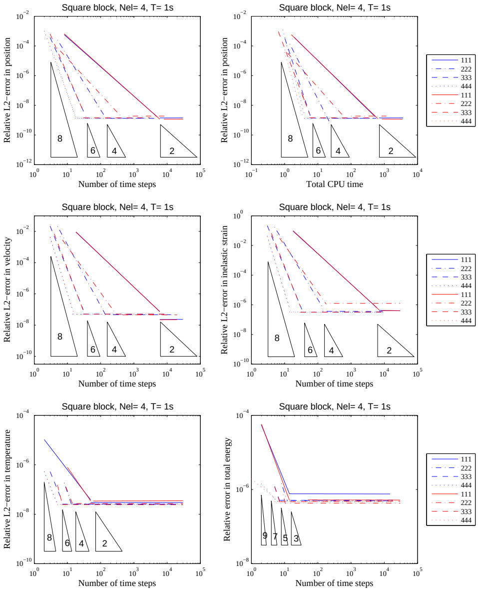

Relative L_2-error of the flying square

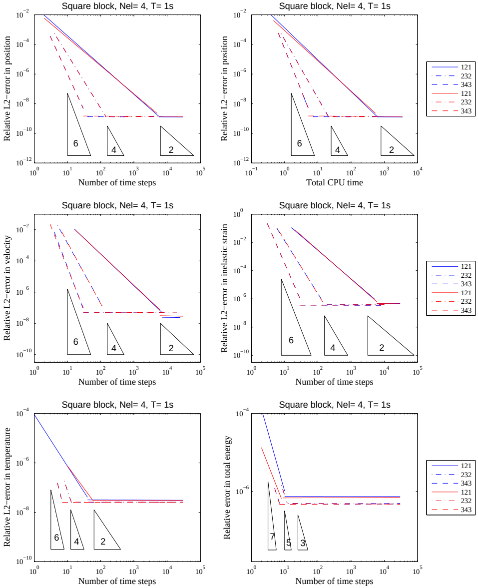

Relative L_2-error of the flying square

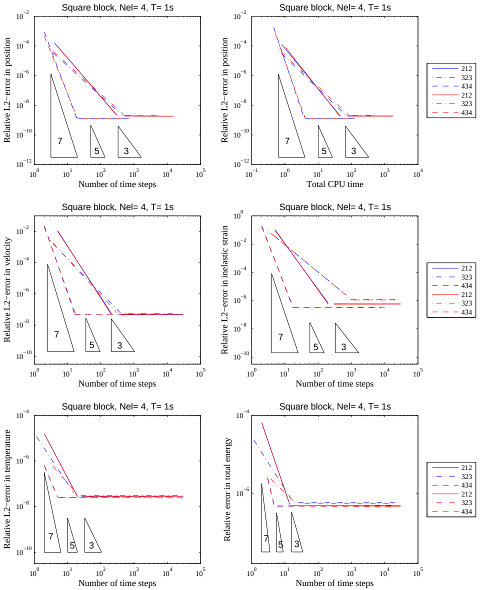

Current configurations of the free flying ring ($k^{\text{mec}} = 2, k^{\text{the}} = 1, k^{\text{vis}} = 2$, method 2)

Inner radius	R_i	$0.5\,\text{cm}$
Outer radius	R_a	$1.5\,\text{cm}$
Thermoviscoelastic Simo-Taylor material		
Mass density	ρ_0	$10\,\text{kg/cm}^2$
First Lamé constant	μ	$7.5\,\text{kJ/cm}^2$
Second Lamé constant	λ	$30\,\text{kJ/cm}^2$
Deviatoric viscosity	V_{dev}	$10\,\text{kJs/cm}^2$
Spherical viscosity	V_{sph}	$50\,\text{kJs/cm}^2$
Specific heat capacity	c	$0.3\,\text{kJ/cm}^2\text{K}$
Heat expansion coefficient	β	$10^{-4}\,\text{K}^{-1}$
Heat conduction coefficient	k_0	$0.3\,\text{kW/K}$
Ambient temperature	Θ_∞	$298.15\,\text{K}$
Global iteration tolerance	tol	$10^{-6}\,\text{J}$
Local iteration tolerance	tolevo	$10^{-10}\,\text{J/cm}^2$
Maximum number of iterations	maxit	10
Number of spatial elements	n_{el}	416
Number of spatial nodes	n_{no}	448

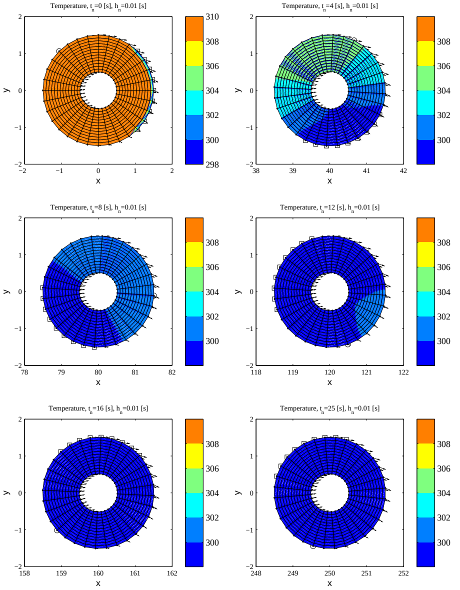

Nodal solution of the free flying ring ($k^{\text{mec}} = 2, k^{\text{the}} = 1, k^{\text{vis}} = 2$, method 2)

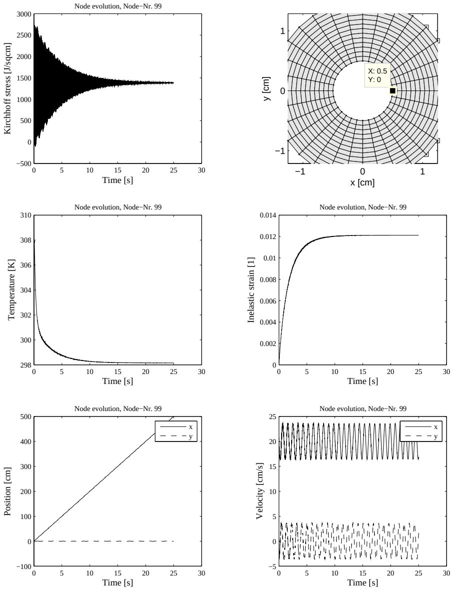

Physical structure of the free flying ring
($k^{\text{mec}} = 2, k^{\text{the}} = 1, k^{\text{vis}} = 2$, method 2)

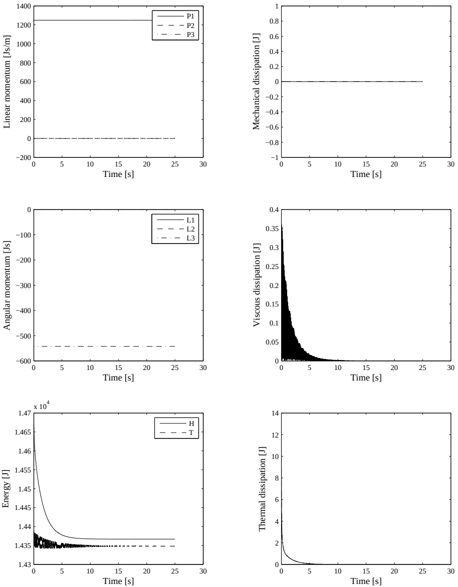

Number of iterations of the free flying ring

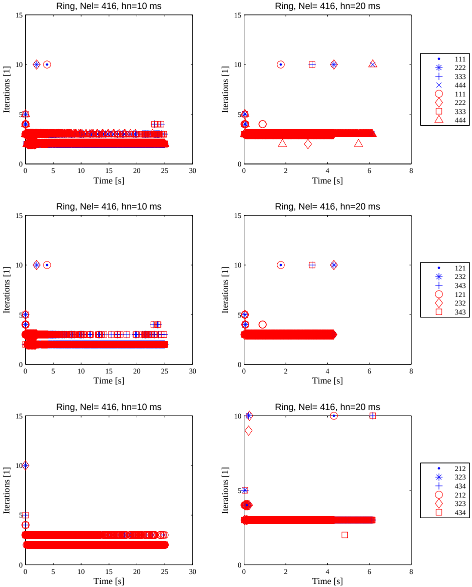

Summary and Outlook

[1]Kuhl & Ramm [1999], Ibrahimbegovic, Chorfi & Gharzeddine [2001], Hartmann, Quint & Arnold [2008]

1. Goal: A stable Galerkin-based time integration method
   - take into account different time scales
   - despite of a monolithic solution strategy
2. Algorithmic basis: The Galerkin-based ehG method
   - energy-momentum consistent
   - higher-order accurate
   - more stable as standard methods
3. Algorithmic upgrade: Multiscale time integration
   - projected entropy approximation (method 1 or method 2)
   - method 1 includes the original ehG method
   - both projections show here comparable accuracy and stability
4. Results: Multiscale time integration with ehG($k_{\mathrm{mec}}, k_{\mathrm{the}}, k_{\mathrm{vis}}$)
   - is able to increase its accuracy order
   - decrease its computational cost (prescribed accuracy)
   - improve its stability (compared to the original ehG(k) method)
5. Outlook: A stable adaptive time integration method [1]